

Leptogenesis from the Dirac CP-violating phase in the minimal left-right symmetric model

Xueke Chen ^a, Xinyi Zhang ^{a,b,c,d} ¹

^a *Department of Physics, Hebei University, Baoding, 071002, China*

^b *Hebei Key Laboratory of High-precision Computation and Application of Quantum Field Theory, Baoding, 071002, China*

^c *Hebei Research Center of the Basic Discipline for Computational Physics, Baoding, 071002, China*

^d *SISSA, International School for Advanced Studies, Via Bonomea 265, 34136 Trieste, Italy*

Abstract

Leptogenesis from low-energy CP violation provides a vital link between neutrino physics and the observed baryon asymmetry of the universe. However, this connection is typically obscured by unknown high-energy parameters. In this work, we investigate thermal leptogenesis in the Minimal Left-Right Symmetric Model with generalized parity as the left-right symmetry, where the hermiticity of the Dirac neutrino coupling allows the right-handed mixing matrix V_R to be determined with minimal assumptions. We show that for a real V_R , these conditions favor CP-conserving Majorana phases, leaving the Dirac CP-violating phase (δ) as the sole source of asymmetry. By numerically exploring all four leptogenesis scenarios, we demonstrate that δ alone can generate the observed baryon asymmetry with the correct sign within specific regions of the parameter space. The results exhibit a high sensitivity to the neutrino mass ordering and the lightest neutrino mass, providing a stringent, testable framework for future experimental measurements of the CP phase and neutrino mass scale.

1 Introduction

Neutrino physics has entered the era of precision measurement. With mixing angles now determined within percent-level uncertainty, the next critical objectives are to resolve the neutrino mass ordering and measure the magnitude of Dirac CP violation [1, 2, 3]. A pressing question in this field is the extent to which low-energy CP violation contributes to the Baryon Asymmetry of the Universe (BAU) via leptogenesis—an elegant and compelling framework for explaining the origin of matter. Exploring this potential link remains a primary frontier at the intersection of particle physics and cosmology. The possibility that the BAU can be accounted for by low-energy CP violation via leptogenesis is particularly intriguing, as it simultaneously addresses the origin of beyond-the-Standard-Model neutrino masses. Furthermore, since traditional seesaw mechanisms for neutrino mass generation typically involve high-energy scales beyond the reach of current colliders, establishing such a connection may provide a rare and vital test for an otherwise inaccessible sector of physics.

The connection between low-energy CP violation and leptogenesis is not straightforward. The neutrino Yukawa coupling—or equivalently the neutrino Dirac mass—governs the CP asymmetry generated by right-handed neutrino (RHN) decays. This coupling receives contributions from both a high-energy sector associated with the heavy RHNs and a low-energy sector associated with the light left-handed neutrinos. In principle, both sectors can contain CP-violating phases that

¹Email: zhangxy@hbu.edu.cn

contribute to the final baryon asymmetry through leptogenesis. To separate these contributions, one can use the Casas-Ibarra parametrization [4], which expresses the neutrino Dirac mass in the fermion mass basis as:

$$M_D = iD_N^{1/2} R D_\nu^{1/2} V_L^\dagger, \quad (1)$$

where D_ν and D_N denote the diagonal mass matrices for light and heavy neutrinos, respectively, and V_L corresponds to the light neutrino mixing matrix. The R matrix is a complex orthogonal matrix that contains potential CP violation from the high-energy sector and parametrizes our ignorance of the neutrino Yukawa coupling. Even if one excludes the specific scenario where contributions from these two sectors cancel out, the unknown high-energy phases can significantly affect the results, limiting our ability to make a definite prediction of the baryon asymmetry arising solely from low-energy CP violation.

Seeking a potential connection between low-energy CP violation and leptogenesis has been a subject of intense investigation for over two decades (e.g., [5, 6, 7, 8, 9, 10]). Existing methods used to identify a possible connection include minimal lepton flavor violation [11, 12], flavor symmetries [13, 14, 15, 16, 17, 18, 19], generalized CP symmetry [20, 21, 18], and quantum corrections [22, 23]. A general connection was first identified in the flavored regime [24, 25], the flavor effect is found to have a non-negligible effect even at extremely high temperatures ($T \gg 10^{12}$ GeV) [26]. Recently, density matrix equations were used to correlate the baryon asymmetry sign with $\sin \delta$ [27]. Furthermore, viable leptogenesis may arise purely from the Dirac CP-violating phase in low-scale freeze-in models [28].

The Minimal Left-Right Symmetric Model (MLRSM) [29, 30, 31, 32] provides a unique framework for pinning down this connection. As pointed out in Refs. [33, 34, 35, 36], the neutrino Yukawa couplings can be completely determined by light and heavy neutrino masses and mixings in the MLRSM when either generalized parity (\mathcal{P}) or charge conjugation (\mathcal{C}) acts as the LR symmetry. This determination eliminates the R -matrix uncertainty, thus providing an excellent pathway for connecting low-energy CP violation to leptogenesis. Furthermore, the MLRSM features rich phenomena concerning neutrinos and leptogenesis. Both Type I and Type II seesaw mechanisms are realized naturally; regarding leptogenesis, the decaying particle can be a triplet scalar in addition to the RHNs. Numerous successful realizations of leptogenesis exist within left-right symmetric theories, focusing on different regimes and methods to constrain the free parameters of the neutrino Yukawa sector [37, 38, 39, 40, 41, 42, 43, 44, 45, 46, 47, 48, 49].

In this work, we investigate the intriguing possibility that the Dirac CP-violating phase is the sole source of CP violation required for unflavored thermal leptogenesis in the MLRSM. The hermiticity of M_D , which follows from the \mathcal{P} transformation, not only helps express the R matrix in terms of light and heavy neutrino masses and mixings but also constrains the parameters of the RHN sector. Utilizing this feature, we make minimal assumptions to produce results with maximal generality. We find that viable Dirac-phase leptogenesis occurs in various MLRSM scenarios within the unflavored regime, in contrast to the Standard Model case.

This paper is organized as follows. In Sec. 2, we set up the basic framework for our discussion. In Sec. 3, we detail how conditions for the V_R parameters arise from the model structure and how the free parameters can be minimized in a meaningful way. In Sec. 4, we present and discuss the numerical results. Finally, we conclude in Sec. 5.

Table 1: Field representations under the gauge groups in MLRSM.

	l_L	l_R	Δ_L	Δ_R	Φ_1	Φ_2
$SU(2)_L$	2	1	3	1	2	2
$SU(2)_R$	1	2	1	3	2	2
$U(1)_{B-L}$	-1	-1	2	2	0	0

2 The framework

The part of the MLRSM Lagrangian relevant to our discussion is

$$\mathcal{L} \supset -\bar{l}_L (Y_1 \Phi_1 - Y_2 \Phi_2^*) l_R - \frac{1}{2} (l_L^T C Y_L i \sigma_2 \Delta_L l_L + l_R^T C Y_R i \sigma_2 \Delta_R l_R) - \lambda_{ij} \text{Tr} (\Delta_R^\dagger \Phi_i \Delta_L \Phi_j^\dagger) + \text{h.c.}, \quad (2)$$

where $i, j = 1, 2$ and

$$l_{L,R} = \begin{pmatrix} \nu \\ e \end{pmatrix}_{L,R}, \quad \Delta_{L,R} = \begin{pmatrix} \delta^+/\sqrt{2} & \delta^{++} \\ \delta^0 & -\delta^+/\sqrt{2} \end{pmatrix}_{L,R}, \quad \Phi_1 = \begin{pmatrix} \phi_1^0 & \phi_2^+ \\ \phi_1^- & -\phi_2^0 \end{pmatrix}, \quad \Phi_2 = \sigma_2 \Phi_1^* \sigma_2. \quad (3)$$

The fields and their representations under the MLRSM gauge group $SU(2)_L \times SU(2)_R \times U(1)_{B-L}$ are shown in Table 1. In addition to these gauge symmetries, the MLRSM features a discrete left-right symmetry—either \mathcal{P} or \mathcal{C} —both of which enforce the equality of the gauge couplings, $g_L = g_R = g$.

The MLRSM gauge symmetry is broken down to the SM gauge symmetry when the neutral component of Δ_R obtains a vacuum expectation value (VEV), $\langle \delta_R^0 \rangle = v_R$. Subsequently, the electroweak symmetry breaks via $\langle \phi_i^0 \rangle = v_i$ (for $i = 1, 2$), which triggers an induced symmetry breaking for Δ_L with $\langle \delta_L^0 \rangle = v_L$. Following the completion of all symmetry-breaking stages, the Lagrangian in Eq. (2) leads to the following neutrino mass terms:

$$\mathcal{L}_\nu \supset -\frac{1}{2} (\bar{\nu}_L^c, \bar{N}_L^c) \mathcal{M} \begin{pmatrix} \nu_L \\ N_L \end{pmatrix} + \text{h.c.}, \quad (4)$$

where we define $N_L \equiv C \bar{\nu}_R$, assuming the hierarchy $v_R \gg v \gg v_L$. The resulting 6×6 effective neutrino mass matrix is:

$$\mathcal{M} = \begin{pmatrix} M_L & M_D^T \\ M_D & M_N \end{pmatrix}, \quad (5)$$

with $M_L = Y_L v_L$, $M_N = Y_R^* v_R$, and $M_D = Y_1 v_1 - Y_2 v_2$. The full 6×6 neutrino mass matrix can be block-diagonalized, from which we obtain the light neutrino mass matrix:

$$M_\nu = M_L - M_D^T \frac{1}{M_N} M_D \equiv M_\nu^{\text{II}} + M_\nu^{\text{I}}. \quad (6)$$

Generally, the light neutrino mass matrix in the MLRSM is composed of both Type-I and Type-II seesaw contributions.

2.1 M_D in MLRSM

The as-yet-unobserved heavy neutrinos interact with SM fields through Yukawa interactions, making these couplings a primary target for experimental probes. More importantly, these interactions

contribute to light neutrino masses, which remain at the frontier of current experimental research. It has been pointed out that in the MLRSM, Yukawa couplings are completely determined by light and heavy neutrino masses and mixings—provided that either \mathcal{C} or \mathcal{P} acts as the LR symmetry and remains unbroken by the VEV of Φ [33, 34, 35, 36]. We briefly review these findings below.

Under the \mathcal{P} transformation, the fields transform as:

$$l_L \leftrightarrow l_R, \Delta_L \leftrightarrow \Delta_R, \Phi \leftrightarrow \Phi^\dagger. \quad (7)$$

Such transformation leads to $Y_{1,2} = Y_{1,2}^\dagger$, $Y_L = Y_R \equiv Y_T$ and further results in

$$M_D = M_D^\dagger \quad (8)$$

in the case of unbroken parity.

To see how M_D can be expressed in terms of light and heavy neutrino masses and mixings, one first writes down the effective light neutrino mass matrix (6) in this scenario:

$$M_\nu = \frac{v_L}{v_R} M_N^* - M_D^T \frac{1}{M_N} M_D. \quad (9)$$

Introducing a matrix H satisfying

$$H H^T \equiv \frac{v_L^*}{v_R} - \frac{1}{\sqrt{M_N}} M_\nu^* \frac{1}{\sqrt{M_N}}, \quad (10)$$

M_D can be written into a compact form

$$M_D = \sqrt{M_N} H \sqrt{M_N^*}, \quad (11)$$

where H is Hermitian, following the hermiticity of M_D . It is clear from Eqs. (10) and (11) that M_D is uniquely determined once the light and heavy neutrino mass matrices are known. Applying these relations to the Type-I seesaw limit (i.e., $M_\nu \simeq M_\nu^I$), one finds:

$$M_D = i \sqrt{M_\nu^* M_N^*}. \quad (12)$$

Under the \mathcal{C} transformation, the fields transform as:

$$l_L \leftrightarrow l_R^c, \Delta_L \leftrightarrow \Delta_R^*, \Phi \leftrightarrow \Phi^T, \quad (13)$$

which leads to $Y_{1,2} = Y_{1,2}^T$, $Y_L = Y_R^* \equiv Y_T$ and consequently

$$M_D = M_D^T. \quad (14)$$

The light neutrino mass matrix is now

$$M_\nu = \frac{v_L}{v_R} M_N - M_D^T \frac{1}{M_N} M_D. \quad (15)$$

Following a similar procedure and exploiting the symmetric nature of M_D in this case, one obtains:

$$M_D = M_N \sqrt{\frac{v_L}{v_R} - \frac{1}{M_N} M_\nu}. \quad (16)$$

The Type-I seesaw limit also results in a compact expression for the Dirac neutrino mass matrix:

$$M_D = i \sqrt{M_N M_\nu}. \quad (17)$$

Table 2: Four possible scenarios of leptogenesis in MLRSM.

	Lepton asymmetry	Neutrino mass
Scenario 1	$m_{N_k} < m_\Delta$	$M_\nu^I > M_\nu^{II}$
Scenario 2	$m_{N_k} < m_\Delta$	$M_\nu^I < M_\nu^{II}$
Scenario 3	$m_{N_k} > m_\Delta$	$M_\nu^I > M_\nu^{II}$
Scenario 4	$m_{N_k} > m_\Delta$	$M_\nu^I < M_\nu^{II}$

2.2 Leptogenesis in MLRSM

MLRSM provides a rich variety of phenomena concerning leptogenesis. In addition to the fact that both Type I and Type II seesaw mechanisms can be naturally realized, the decaying particle responsible for generating lepton number asymmetry can be the left-handed triplet as well as the RHNs. Consequently, there are four possible scenarios considering unflavored thermal leptogenesis, which we list in Table 2.

In Scenarios 1 and 2, RHNs are the decaying particles responsible for generating the CP asymmetry. In addition to the standard loop diagrams, the MLRSM includes a supplemental diagram featuring a triplet in the loop, which further contributes to the CP asymmetry [50]

$$\epsilon_{N_k}^\Delta = -\frac{1}{2\pi} \frac{\sum_{il} \text{Im} [(Y_N)_{ki} (Y_N)_{kl} (Y_T^*)_{il} \mu]}{\sum_i |(Y_N)_{ki}|^2 m_{N_k}} \left[1 - \frac{m_\Delta^2}{m_{N_k}^2} \ln \left(1 + \frac{m_{N_k}^2}{m_\Delta^2} \right) \right]. \quad (18)$$

Note that $\epsilon_{N_k}^\Delta$ does not have the usual $Y_N Y_N^\dagger$ dependence found in the conventional CP asymmetry ϵ_{N_k} . Consequently, the left-handed mixing is not cancelled out, allowing low-energy CP violation to persist even in the unflavored regime ($T > 10^{12}$ GeV). In this regime, the Boltzmann equations governing the evolution are

$$\begin{aligned} \frac{dY_{N_i}}{dz} &= \frac{-z}{sH} (\gamma_D^i + \gamma_{S,\Delta L=1}^i) \left(\frac{Y_{N_i}}{Y_{N_i}^{\text{eq}}} - 1 \right); \\ \frac{dY_\Delta}{dz} &= \frac{-z}{sH} \left[\sum_{i=1}^3 \epsilon_i (\gamma_D^i + \gamma_{S,\Delta L=1}^i) \left(\frac{Y_{N_i}}{Y_{N_i}^{\text{eq}}} - 1 \right) - \left(\frac{\gamma_D^i}{2} + \gamma_{W,\Delta L=1}^i \right) \frac{Y_\Delta}{Y_l^{\text{eq}}} \right], \end{aligned} \quad (19)$$

where Y_{N_i} is the N_i abundance ($Y_{N_i}^{\text{eq}}$ is the equilibrium abundance), $Y_\Delta \equiv Y_{\Delta B}/3 - Y_{\Delta L}$, and $\epsilon_i \equiv \epsilon_{N_i} + \epsilon_{N_i}^\Delta$. Here, the various γ denote the reaction rates (or rate densities) with subscripts indicating the respective processes.

In Scenarios 3 and 4, the triplet is lighter than the RHNs, and the CP asymmetry is generated through triplet decay as:

$$\epsilon_\Delta = \frac{1}{8\pi} \sum_k m_{N_k} \frac{\sum_{il} \text{Im} [(Y_N^*)_{ki} (Y_N^*)_{kl} (Y_T)_{il} \mu^*]}{\sum_{ij} |(Y_T)_{ij}|^2 m_\Delta^2 + |\mu|^2} \ln \left(1 + \frac{m_\Delta^2}{m_{N_k}^2} \right). \quad (20)$$

For $T > 10^{12}$ GeV, neglecting spectator processes, the Boltzmann equations in these scenarios are given by [51]:

$$\begin{aligned} sH z \frac{d\Sigma_\Delta}{dz} &= - \left(\frac{\Sigma_\Delta}{\Sigma_\Delta^{\text{eq}}} - 1 \right) \gamma_D - 2 \left[\left(\frac{\Sigma_\Delta}{\Sigma_\Delta^{\text{eq}}} \right)^2 - 1 \right] \gamma_A; \\ sH z \frac{d\Delta_\Delta}{dz} &= - \left(\frac{\Delta_\Delta}{\Sigma_\Delta^{\text{eq}}} - B_l \frac{Y_\Delta}{Y_l^{\text{eq}}} + B_H \frac{Y_\Delta + 2\Delta_\Delta}{Y_H^{\text{eq}}} \right) \gamma_D; \\ sH z \frac{dY_\Delta}{dz} &= - \left(\frac{\Sigma_\Delta}{\Sigma_\Delta^{\text{eq}}} - 1 \right) \gamma_D \epsilon_\Delta - 2B_l \left(\frac{dY_\Delta}{Y_l^{\text{eq}}} - \frac{\Delta_\Delta}{\Sigma_\Delta^{\text{eq}}} \right) \gamma_D - 2 \left(\frac{Y_\Delta}{Y_l^{\text{eq}}} + \frac{Y_\Delta + 2\Delta_\Delta}{Y_H^{\text{eq}}} \right) \gamma_{lH}, \end{aligned} \quad (21)$$

where $\Sigma_\Delta \equiv (n_\Delta + n_{\bar{\Delta}})/s$ and $\Delta_\Delta \equiv (n_\Delta - n_{\bar{\Delta}})/s$ represent the total triplet abundance and asymmetry, respectively, while $B_l \equiv \text{BR}(\Delta \rightarrow \bar{l}l)$ and $B_H \equiv \text{BR}(\Delta \rightarrow HH)$ are the branching ratios.

3 Conditions for V_R parameters

3.1 Unknown V_R and constraining conditions

Despite the fact that the MLRSM model with discrete parity or charge conjugation symmetries allows for the determination of M_D , fully determining M_D requires knowledge of the heavy neutrino mixing matrix, V_R , which is unknown a priori. In the literature, the V_R matrix is generally taken to be the identity matrix [52], to coincide with V_L [47], or to be parameterized in relation to V_L [53, 54].

In Ref. [36], it is pointed out that the H matrix in Eq. (11) inherits hermiticity from M_D , which further implies $\text{ImTr}(HH^T)^n = 0$, ($n = 1, 2, 3$). This serves as a set of constraint conditions for V_R parameters (and V_L parameters) when expressed using Eq. (10)

$$\text{ImTr} \left[\frac{v_L^*}{v_R} - \frac{1}{M_N} M_\nu^* \right]^n = 0, \quad n = 1, 2, 3 \quad (22)$$

Mathematically, these conditions are equivalent to the requirement that the coefficients of the characteristic polynomial of the HH^T matrix be real, which implies that the eigenvalues of HH^T must be either real or occur in complex conjugate pairs. These conditions correlate the phases of both the left- and right-handed mixing matrices and serve as constraints on the V_R parameters.

However, these conditions involve a large number of parameters. Even if we fix the dimensionful parameters (v_L , v_R , and the heavy and light neutrino masses), we are left with twelve parameters in the mixing matrices alone. Using the best-fit values for left-handed mixing still leaves eight degrees of freedom. Generally, there are six parameters in V_R : three mixing angles (γ_{ij}), one Dirac phase, and two Majorana phases. Since there are far fewer equations than parameters, we expect a large degeneracy in the parameter space; namely, for a fixed set of V_L parameters, there is an infinite set of V_R parameters satisfying the conditions. Such a situation is certainly daunting for proceeding with the baryogenesis calculation.

Meanwhile, it should be noted that the left-hand sides of the three conditions are exceedingly complicated. Even the simplest condition contains 99 terms, with a total of 2,443 indivisible subexpressions. For the final condition, there are 56,166 terms and 2,018,024 subexpressions. Given this complexity, and the fact that we are primarily interested in the role of low-energy CP-violating parameters, we choose to set all phases in the V_R sector to zero. This leaves us with three variables, which can then be readily solved using the three equations.

It should be noted that the constraint conditions follow directly from the hermiticity of H , which in turn follows from the hermiticity of M_D . When \mathcal{C} is the LR symmetry, M_D is symmetric instead of hermitian, leading to no similar constraints. In other words, V_R is unconstrained in that case. Given the large number of free parameters, we choose to work exclusively with the case where \mathcal{P} is the LR symmetry.

3.2 Real V_R and phases of V_L

We first consider the scenario where only the Dirac CP phase is nonzero. The imaginary part of the trace of HH^T arises solely from the presence of this Dirac phase. By adjusting the three mixing angles in V_R , one can effectively rotate the generations to find a real trace. To illustrate

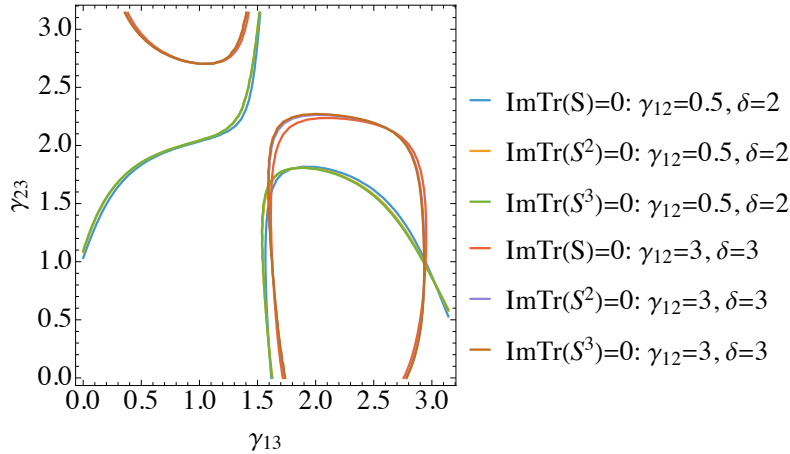


Figure 1: The real-trace contours ($\text{ImTr}(S^n) = 0$ for $n = 1, 2, 3$) are plotted for two V_R mixing angles, using two sets of randomly chosen values for γ_{12} and δ . The intersection of the three lines (for a given set of inputs) indicates a simultaneous solution to the three constraints.

that such a solution exists, we plot the contours of the real trace of $S \equiv HH^T$ for two sets of randomly chosen values for γ_{12} and δ in Figure 1. The intersection of the three lines indicates a simultaneous solution. As shown, in both cases, the three contour lines intersect.

Next, we include the Majorana phases of V_L . We fix V_R to be V_L , the identity matrix, or a set of arbitrarily chosen mixing angles, while allowing the two Majorana phases of V_L to vary in the range $[0, 2\pi]$. Upon computing the imaginary parts of the traces of S^n for $n = 1, 2, 3$, the results are shown in Figure 2. We find that $\text{ImTr}(S)$ approaches zero as $\alpha_{31} \rightarrow n\pi$. For $\text{ImTr}(S^2)$, this occurs at $\alpha_{31} = n\pi/2$, and for $\text{ImTr}(S^3)$, at $\alpha_{31} = n\pi/4$. Consequently, to simultaneously satisfy all three conditions, we must choose $\alpha_{31} = n\pi$. No similar behavior was observed for α_{21} .

Following the indications from the above results, we set $\alpha_{31} = n\pi$. We then vary α_{21} and γ_{ij} randomly and plot $\text{ImTr}(S^n)$, $n = 1, 2, 3$. The results are shown in Figure 3. From this figure, we see that while the behavior is less decisive for $\text{ImTr}(S^2)$ and $\text{ImTr}(S^3)$, $\text{ImTr}(S)$ approaches zero when α_{21} takes the CP-conserving values $n\pi$, regardless of the values of γ_{ij} .

The results above motivate our choice to work with a real V_R and vanishing Majorana phases for V_L . These results can be understood by considering the different positions of the Dirac and Majorana CP-violating phases. The Dirac phase is inter-generational; in this case, it is easier for the V_R angles to rotate into a basis with a real trace. In contrast, the Majorana phases are intrinsic to the mass eigenstates. Since a real V_R can only redistribute the weights of different mass eigenstates, if these weights do not align perfectly to cancel the phases, a real trace cannot be found. It is worth stressing that the CP-conserving tendency of the two V_L Majorana phases arises when V_R is real. Once phases are allowed to enter V_R , non-zero phases in V_L must balance the effect to satisfy the real-trace conditions.

4 Numeric results

4.1 Overview of parameters and inputs

To actually solve for V_R using the constraints in Eq. (22), we need to specify the values of all other parameters. The model parameters can be categorized as follows:

- Dimensionful parameters: heavy and light neutrino masses, the triplet mass m_Δ , and the VEVs v_L and v_R .

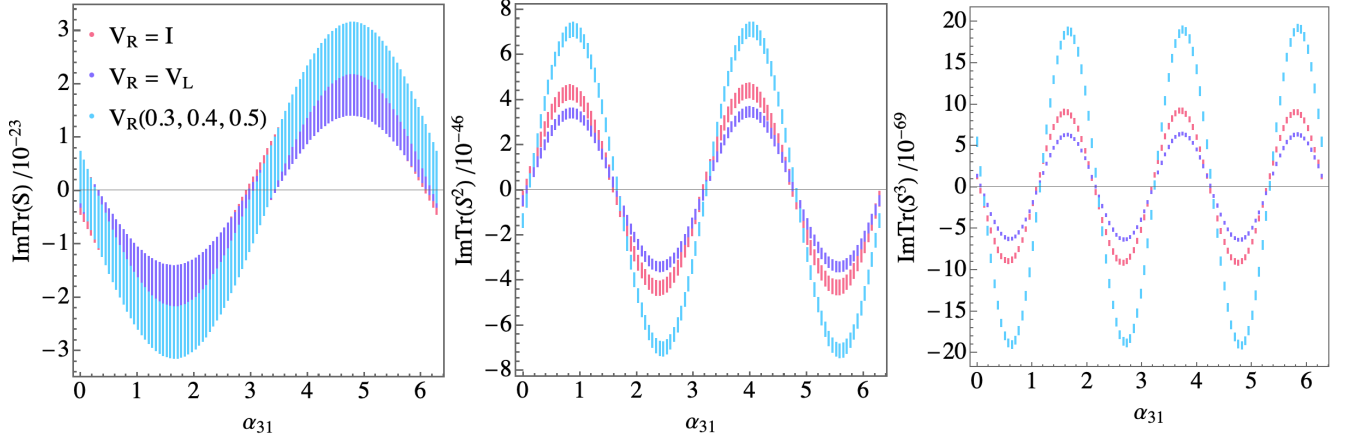


Figure 2: Values of $\text{ImTr}(S^n)$ for $n = 1, 2, 3$ are calculated using randomly sampled values of α_{31} and α_{21} for three different choices of real V_R . The “ $V_R = V_L$ ” case refers to a real V_R matrix with mixing angles equal to those of V_L .

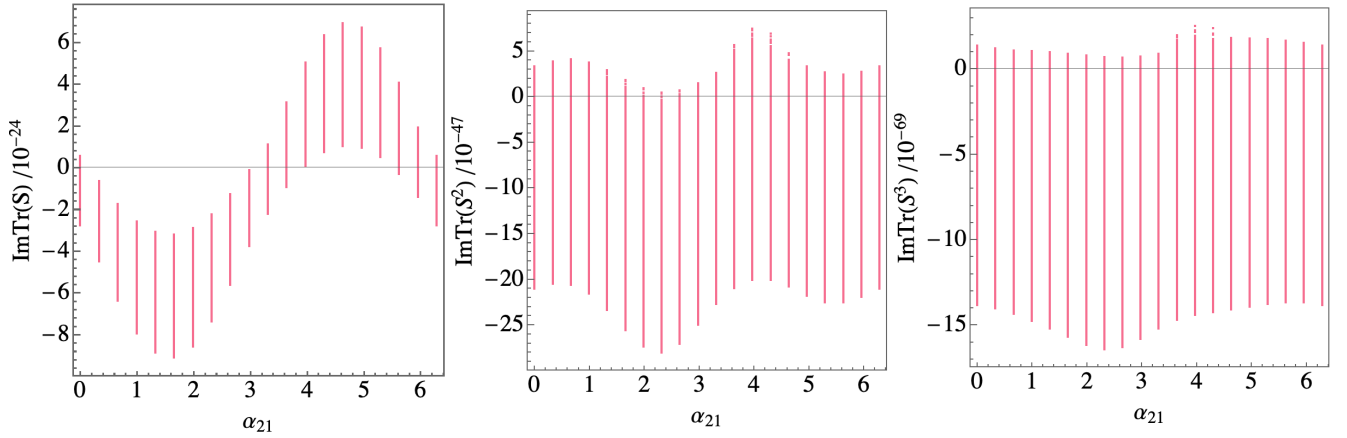


Figure 3: Values of $\text{ImTr}(S^n)$ for $n = 1, 2, 3$, calculated using randomly sampled values of α_{21} and V_R mixing angles, with α_{31} fixed to $n\pi$.

- Dimensionless parameters: mixing angles and phases in both the left- and right-handed mixing matrices.

Generally speaking, due to the significantly larger uncertainty in the dimensionful parameters, varying them leads to more pronounced changes in the results. For hierarchical RHNs, the RHN mass is proportional to the CP asymmetry, which leads to the Davidson-Ibarra bound [55]. A critical threshold for m_{N_k} occurs when $m_{N_k} < 10^{12}$ GeV (and 10^9 GeV); at such scales, specific Yukawa interactions enter equilibrium and become distinguishable, meaning flavor effects can no longer be neglected [56]. Another interesting possibility arises when the heavy neutrino mass spectrum is nearly degenerate, leading to a resonant enhancement of the CP asymmetry [57]. Numerical examples illustrating the effects of varying these dimensionful parameters can be found in Ref. [46] (see Figs. 4 and 9 for m_{N_k} and m_Δ , and Fig. 19 for different heavy neutrino mass spectra). From these results, we find that for heavy neutrino mass spectra that are neither degenerate nor highly hierarchical, the impact on the resulting baryon asymmetry is limited. We fix the heavy neutrino mass spectrum to be $m_{N_2} = 2m_{N_1}$ and $m_{N_3} = 3m_{N_1}$, and include the contributions from all RHNs.

The dimensionless parameters serve to redistribute the influence of the dimensionful quanti-

Table 3: Dimensionful parameters input.

	m_{N_1} [GeV]	m_Δ [GeV]	v_L/v_R
Scenario 1	10^{12}	10^{14}	10^{-25}
Scenario 2	10^{12}	5×10^{13}	1.45×10^{-23}
Scenario 3	10^{14}	5×10^{12}	10^{-27}
Scenario 4	10^{14}	5×10^{12}	1.45×10^{-25}

ties. This redistribution effect can be quite sharp—potentially driving the CP asymmetries, and consequently the baryon asymmetry, to zero. Fixing the dimensionful parameters allows one to trace the variations of the dimensionless parameters more clearly; in our case, this isolates the effects of the Dirac CP-violating phase. In our numerical study, we fix the left-handed mixing angles to their best-fit values while allowing the Dirac CP-violating phase to vary.

Since this work makes no assumptions regarding the V_R parameters—which already greatly enlarges the parameter space—we choose to fix the dimensionful parameters to the benchmark values shown in Table 3. Once the mass of the decaying particle is chosen, the ratio of the VEVs (v_L/v_R) is constrained by the mass contribution conditions corresponding to the four scenarios. Fixing these dimensionful parameters allows us to focus exclusively on the effects of Dirac CP violation. Furthermore, as long as the masses do not enter specific regimes (namely the flavored or resonant regimes), one expects similar behavior at other mass scales.

4.2 Numeric results and discussions

We select three benchmark values for the lightest neutrino mass: $m_{\min} = 0.0001, 0.001, 0.01$ eV, while sampling the Dirac CP-violating phase evenly in the range $[0, 2\pi]$. The Boltzmann equations in Eqs. (19) and (21) are employed to calculate the baryon asymmetry for the four scenarios under both light neutrino mass orderings. In Figure 4, we plot the predicted baryon asymmetry as a function of the Dirac CP-violating phase for each scenario.

A primary observation from Figure 4 is that the predicted curves do not exhibit a simple oscillatory or sinusoidal dependence on δ . This is expected, as each point in the parameter space corresponds to distinct values of the RHN mixing γ_{ij} determined through the hermiticity conditions in Eq. (22).

We display only the regions where Y_B carries the correct sign and show observational constraints on Y_B and δ as color-shaded bands. The “blank” regions—visible, for instance, in scenario S3(IO)—correspond to parameter space points yielding negative Y_B values. For our chosen benchmark values of m_{\min} , we find several intersections with the experimental Y_B band where the observed asymmetry is successfully reproduced. While some of these intersections fall outside the 3σ (or 1σ) confidence levels for δ (shaded in yellow), every scenario overlaps with at least the 3σ favored region. This confirms that feasible solutions satisfying both cosmological and oscillation constraints exist across all considered cases.

It is evident that no universal behavior governs these scenarios; the curves vary significantly with m_{\min} , the mass ordering, and the specific leptogenesis scenario. This underscores the high sensitivity of the baryon asymmetry to the lightest neutrino mass and the mass ordering. Notably, the dependence on the Dirac CP-violating phase is remarkably sharp. For a fixed m_{\min} , varying δ can shift Y_B by one (e.g., S4(NO)) to two orders of magnitude (e.g., S2(NO) and S3(NO)). Such sensitivity ensures that leptogenesis in these models will provide a stringent test for future high-precision measurements of δ .

Our results provide a consistent mapping from the (δ, m_{\min}) plane to the final baryon asymmetry for a given scale of the heavy decaying particle, m_H . Although this study was conducted with a fixed m_H for each scenario, the underlying framework remains general. As future experiments continue to constrain the light neutrino sector, it will be possible to invert this relationship: by utilizing the observed baryon asymmetry as a benchmark, one could potentially probe or constrain the mass scale m_H itself. This is particularly significant given that these high-energy scales are generally beyond the direct reach of current and planned collider experiments.

5 Conclusions

Leptogenesis arising from low-energy CP violation provides a compelling bridge between the fundamental properties of neutrinos and the evolution of the early universe. While a direct connection is often obscured by the unknown parameters of the high-energy sector, the MLRSM offers a structured framework to link these scales.

In this work, we have investigated leptogenesis with minimal assumptions by determining the V_R parameters through conditions enforced by the hermiticity of the neutrino Dirac Yukawa coupling under the \mathcal{P} transformation. We find that these real trace conditions favor CP-conserving values for the Majorana phases, effectively leaving the Dirac CP-violating phase as the only source of the asymmetry. By numerically exploring all four possible leptogenesis scenarios within this framework, we demonstrate that viable leptogenesis is achievable, generating the observed baryon asymmetry with the correct sign.

Our results demonstrate that the final baryon asymmetry is highly sensitive to the Dirac CP-violating phase δ , the neutrino mass ordering, and the absolute mass scale m_{\min} . This sensitivity provides a clear path for testing leptogenesis in the MLRSM against upcoming experimental data. By avoiding ad-hoc assumptions regarding neutrino Yukawa couplings and minimizing free parameters, our approach establishes a robust mapping from the (m_{\min}, δ) plane to the observed cosmic matter-antimatter asymmetry for a given high-energy scale m_H .

As future experiments like DUNE, JUNO, and Hyper-K continue to constrain the light neutrino sector, these results will allow us to more precisely evaluate the feasibility of thermal leptogenesis in MLRSM. Furthermore, by anchoring our model to the observed baryon asymmetry, this framework allows us to invert the logic: we can potentially probe the heavy mass scale m_H , which remains otherwise beyond the direct reach of current and planned collider experiments. Ultimately, this work provides a consistent mapping that could eventually narrow the allowed range of the lightest neutrino mass while offering insights into the high-energy completion of the lepton sector.

Acknowledgements

XYZ would like to thank Jiang-Hao Yu for suggesting this research in the first place and for early collaboration. The authors would like to thank Gang Li for helpful conversations. This work is supported by National Natural Science Foundation of China under grant No.12305116, Start-up Funds for Young Talents of Hebei University (No.521100223012). XYZ is also supported by the China Scholarship Council (CSC).

References

- [1] JUNO collaboration, *Neutrino Physics with JUNO*, *J. Phys. G* **43** (2016) 030401 [1507.05613].

- [2] DUNE collaboration, *Long-Baseline Neutrino Facility (LBNF) and Deep Underground Neutrino Experiment (DUNE): Conceptual Design Report, Volume 2: The Physics Program for DUNE at LBNF*, 1512.06148.
- [3] HYPER-KAMIOKANDE collaboration, *Hyper-Kamiokande Design Report*, 1805.04163.
- [4] J.A. Casas and A. Ibarra, *Oscillating neutrinos and $\mu \rightarrow e, \gamma$* , *Nucl. Phys. B* **618** (2001) 171 [hep-ph/0103065].
- [5] G.C. Branco, T. Morozumi, B.M. Nobre and M.N. Rebelo, *A Bridge between CP violation at low-energies and leptogenesis*, *Nucl. Phys. B* **617** (2001) 475 [hep-ph/0107164].
- [6] S. Davidson and A. Ibarra, *Leptogenesis and low-energy phases*, *Nucl. Phys. B* **648** (2003) 345 [hep-ph/0206304].
- [7] P.H. Frampton, S.L. Glashow and T. Yanagida, *Cosmological sign of neutrino CP violation*, *Phys. Lett. B* **548** (2002) 119 [hep-ph/0208157].
- [8] T. Endoh, S. Kaneko, S.K. Kang, T. Morozumi and M. Tanimoto, *CP violation in neutrino oscillation and leptogenesis*, *Phys. Rev. Lett.* **89** (2002) 231601 [hep-ph/0209020].
- [9] G.C. Branco, R. Gonzalez Felipe, F.R. Joaquim, I. Masina, M.N. Rebelo and C.A. Savoy, *Minimal scenarios for leptogenesis and CP violation*, *Phys. Rev. D* **67** (2003) 073025 [hep-ph/0211001].
- [10] S. Pascoli, S.T. Petcov and W. Rodejohann, *On the connection of leptogenesis with low-energy CP violation and LFV charged lepton decays*, *Phys. Rev. D* **68** (2003) 093007 [hep-ph/0302054].
- [11] G.C. Branco, A.J. Buras, S. Jager, S. Uhlig and A. Weiler, *Another look at minimal lepton flavour violation, $l_i \rightarrow l_j \gamma$, leptogenesis, and the ratio M_ν/Λ_{LFV}* , *JHEP* **09** (2007) 004 [hep-ph/0609067].
- [12] L. Merlo and S. Rosauero-Alcaraz, *Predictive Leptogenesis from Minimal Lepton Flavour Violation*, *JHEP* **07** (2018) 036 [1801.03937].
- [13] C. Hagedorn, E. Molinaro and S.T. Petcov, *Majorana Phases and Leptogenesis in See-Saw Models with $A(4)$ Symmetry*, *JHEP* **09** (2009) 115 [0908.0240].
- [14] A. Meroni, E. Molinaro and S.T. Petcov, *Revisiting Leptogenesis in a SUSY $SU(5) \times T'$ Model of Flavour*, *Phys. Lett. B* **710** (2012) 435 [1203.4435].
- [15] B. Karmakar and A. Sil, *Nonzero ν_{13} and leptogenesis in a type-I seesaw model with A_4 symmetry*, *Phys. Rev. D* **91** (2015) 013004 [1407.5826].
- [16] J. Gehrlein, S.T. Petcov, M. Spinrath and X. Zhang, *Leptogenesis in an $SU(5) \times A_5$ Golden Ratio Flavour Model*, *Nucl. Phys. B* **896** (2015) 311 [1502.00110].
- [17] T. Ishihara, N. Maekawa, M. Takegawa and M. Yamanaka, *Leptogenesis in $E_6 \times U(1)_A$ SUSY GUT model*, *JHEP* **02** (2016) 108 [1508.06212].
- [18] C.-C. Li and G.-J. Ding, *Implications of residual CP symmetry for leptogenesis in a model with two right-handed neutrinos*, *Phys. Rev. D* **96** (2017) 075005 [1701.08508].

- [19] M. Drewes, Y. Georis, C. Hagedorn and J. Klarić, *Low-scale leptogenesis with flavour and CP symmetries*, *JHEP* **12** (2022) 044 [2203.08538].
- [20] P. Chen, G.-J. Ding and S.F. King, *Leptogenesis and residual CP symmetry*, *JHEP* **03** (2016) 206 [1602.03873].
- [21] C. Hagedorn and E. Molinaro, *Flavor and CP symmetries for leptogenesis and $0\nu\beta\beta$ decay*, *Nucl. Phys. B* **919** (2017) 404 [1602.04206].
- [22] Z.-z. Xing and D. Zhang, *A direct link between unflavored leptogenesis and low-energy CP violation via the one-loop quantum corrections*, *JHEP* **04** (2020) 179 [2003.00480].
- [23] Z.-z. Xing and D. Zhang, *Bridging resonant leptogenesis and low-energy CP violation with an RGE-modified seesaw relation*, *Phys. Lett. B* **804** (2020) 135397 [2003.06312].
- [24] S. Pascoli, S.T. Petcov and A. Riotto, *Connecting low energy leptonic CP-violation to leptogenesis*, *Phys. Rev. D* **75** (2007) 083511 [hep-ph/0609125].
- [25] S. Pascoli, S.T. Petcov and A. Riotto, *Leptogenesis and Low Energy CP Violation in Neutrino Physics*, *Nucl. Phys. B* **774** (2007) 1 [hep-ph/0611338].
- [26] K. Moffat, S. Pascoli, S.T. Petcov and J. Turner, *Leptogenesis from Low Energy CP Violation*, *JHEP* **03** (2019) 034 [1809.08251].
- [27] A. Granelli, K. Moffat and S.T. Petcov, *Aspects of high scale leptogenesis with low-energy leptonic CP violation*, *JHEP* **11** (2021) 149 [2107.02079].
- [28] A. Granelli, S. Pascoli and S.T. Petcov, *Low-Scale Leptogenesis with Low-Energy Dirac CP-Violation*, *Phys. Rev. D* **108** (2023) L101302 [2307.07476].
- [29] J.C. Pati and A. Salam, *Lepton Number as the Fourth Color*, *Phys. Rev. D* **10** (1974) 275.
- [30] R.N. Mohapatra and J.C. Pati, *A Natural Left-Right Symmetry*, *Phys. Rev. D* **11** (1975) 2558.
- [31] G. Senjanovic and R.N. Mohapatra, *Exact Left-Right Symmetry and Spontaneous Violation of Parity*, *Phys. Rev. D* **12** (1975) 1502.
- [32] G. Senjanovic, *Spontaneous Breakdown of Parity in a Class of Gauge Theories*, *Nucl. Phys. B* **153** (1979) 334.
- [33] M. Nemevsek, G. Senjanovic and V. Tello, *Connecting Dirac and Majorana Neutrino Mass Matrices in the Minimal Left-Right Symmetric Model*, *Phys. Rev. Lett.* **110** (2013) 151802 [1211.2837].
- [34] G. Senjanović and V. Tello, *Probing Seesaw with Parity Restoration*, *Phys. Rev. Lett.* **119** (2017) 201803 [1612.05503].
- [35] G. Senjanovic and V. Tello, *Disentangling the seesaw mechanism in the minimal left-right symmetric model*, *Phys. Rev. D* **100** (2019) 115031 [1812.03790].
- [36] G. Senjanovic and V. Tello, *Parity and the origin of neutrino mass*, *Int. J. Mod. Phys. A* **35** (2020) 2050053 [1912.13060].

- [37] A.S. Joshipura, E.A. Paschos and W. Rodejohann, *Leptogenesis in left-right symmetric theories*, *Nucl. Phys. B* **611** (2001) 227 [[hep-ph/0104228](#)].
- [38] W. Rodejohann and K.R.S. Balaji, *Leptogenesis and low-energy observables in left-right symmetric models*, *Phys. Rev. D* **65** (2002) 093009 [[hep-ph/0201052](#)].
- [39] K.S. Babu, A. Bachri and H. Aissaoui, *Leptogenesis in minimal left-right symmetric models*, *Nucl. Phys. B* **738** (2006) 76 [[hep-ph/0509091](#)].
- [40] E.K. Akhmedov, M. Blennow, T. Hallgren, T. Konstandin and T. Ohlsson, *Stability and leptogenesis in the left-right symmetric seesaw mechanism*, *JHEP* **04** (2007) 022 [[hep-ph/0612194](#)].
- [41] W. Chao, S. Luo and Z.-z. Xing, *Neutrino mixing and leptogenesis in type-II seesaw scenarios with left-right symmetry*, *Phys. Lett. B* **659** (2008) 281 [[0704.3838](#)].
- [42] T. Hallgren, T. Konstandin and T. Ohlsson, *Triplet Leptogenesis in Left-Right Symmetric Seesaw Models*, *JCAP* **01** (2008) 014 [[0710.2408](#)].
- [43] A. Abada, P. Hosteins, F.-X. Josse-Michaux and S. Lavignac, *Successful Leptogenesis in $SO(10)$ Unification with a Left-Right Symmetric Seesaw Mechanism*, *Nucl. Phys. B* **809** (2009) 183 [[0808.2058](#)].
- [44] P.-H. Gu, *New leptogenesis scenario parametrized by Dirac neutrino mass matrix*, *Phys. Rev. D* **96** (2017) 075024 [[1410.5753](#)].
- [45] T. Rink, W. Rodejohann and K. Schmitz, *Leptogenesis and low-energy CP violation in a type-II-dominated left-right seesaw model*, *Nucl. Phys. B* **972** (2021) 115552 [[2006.03021](#)].
- [46] X. Zhang, J.-H. Yu and B.-Q. Ma, *Leptogenesis from low-energy CP violation in minimal left-right symmetric model*, *Nucl. Phys. B* **976** (2022) 115670 [[2008.06433](#)].
- [47] U. Patel, P. Adarsh, S. Patra and P. Sahu, *Leptogenesis in a Left-Right Symmetric Model with double seesaw*, *JHEP* **03** (2024) 029 [[2310.09337](#)].
- [48] K.S. Babu and A. Kaladharan, *Dirac leptogenesis in left-right symmetric models*, *Phys. Rev. D* **112** (2025) 035015 [[2410.24125](#)].
- [49] B. Kumar and M.K. Das, *Leptogenesis, $0\nu\beta\beta$ and lepton flavor violation in modular left-right asymmetric model with polyharmonic $M_{\alpha\beta}$ forms*, *JHEP* **09** (2025) 071 [[2504.21701](#)].
- [50] T. Hambye and G. Senjanovic, *Consequences of triplet seesaw for leptogenesis*, *Phys. Lett. B* **582** (2004) 73 [[hep-ph/0307237](#)].
- [51] S. Lavignac and B. Schmauch, *Flavour always matters in scalar triplet leptogenesis*, *JHEP* **05** (2015) 124 [[1503.00629](#)].
- [52] P.S.B. Dev, J. Heeck and A. Thapa, *Decaying scalar dark matter in the minimal left-right symmetric model*, *Phys. Rev. D* **112** (2025) 015004 [[2501.14669](#)].
- [53] G. Li, D.-Y. Luo and X. Zhao, *Calculable neutrino Dirac mass matrix and one-loop θ^- in the minimal left-right symmetric model*, *Phys. Rev. D* **110** (2024) 035030 [[2404.16740](#)].

- [54] O. Mikulenko, *Quasi-degenerate heavy neutral leptons in the left-right symmetric model*, *JHEP* **06** (2025) 023 [2406.13850].
- [55] S. Davidson and A. Ibarra, *A Lower bound on the right-handed neutrino mass from leptogenesis*, *Phys. Lett. B* **535** (2002) 25 [hep-ph/0202239].
- [56] S. Blanchet and P. Di Bari, *Flavor effects on leptogenesis predictions*, *JCAP* **03** (2007) 018 [hep-ph/0607330].
- [57] A. Pilaftsis and T.E.J. Underwood, *Electroweak-scale resonant leptogenesis*, *Phys. Rev. D* **72** (2005) 113001 [hep-ph/0506107].
- [58] I. Esteban, M.C. Gonzalez-Garcia, M. Maltoni, I. Martinez-Soler, J.P. Pinheiro and T. Schwetz, *NuFit-6.0: updated global analysis of three-flavor neutrino oscillations*, *JHEP* **12** (2024) 216 [2410.05380].

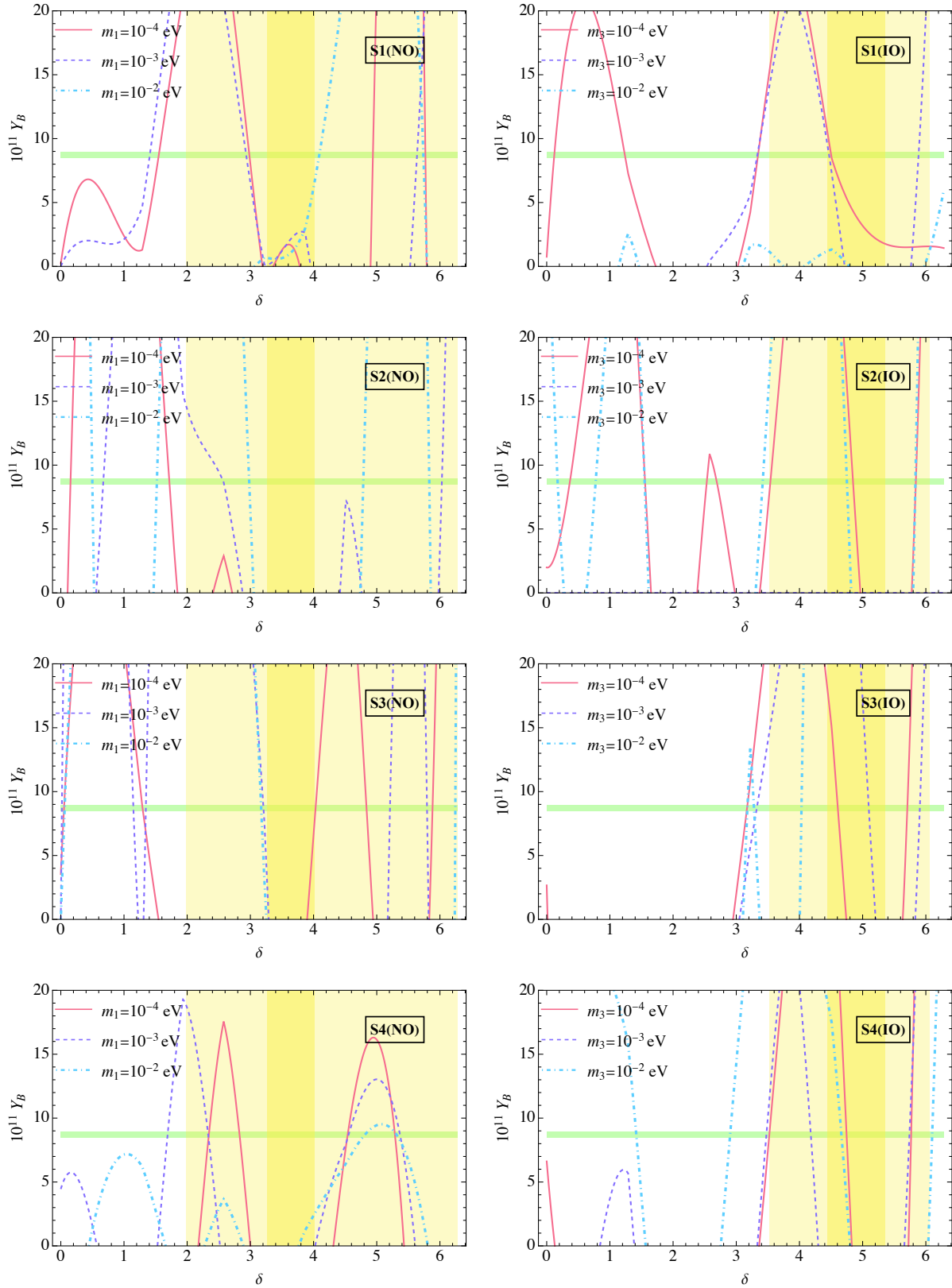


Figure 4: Predicted values of the baryon asymmetry as a function of the Dirac CP-violating phase for both mass orderings of light neutrinos in each scenario (labeled S1 through S4). The left panel corresponds to normal ordering (NO), while the right panel corresponds to inverted ordering (IO). In each plot, three benchmark values of the lightest neutrino mass are shown. The green shaded region represents the 3σ experimental bound on the baryon asymmetry, while the light yellow shaded region indicates the 3σ range for δ from NuFIT 6.1 [58], with the darker yellow sub-region representing the 1σ range.